

Structure of Semibullvalene in the Gas Phase

Y. C. Wang and S. H. Bauer*

Contribution from the Department of Chemistry, Cornell University, Ithaca, New York 14850. Received November 29, 1971

Abstract: The structure of tricyclo[3.3.0.0^{2,8}]octa-3,6-diene in the gas phase was investigated by electron diffraction. Three sets of photographs were taken to cover the range in q from 5 to 150 Å⁻¹. With a newly developed program for an augmented DEC-PDP-9 computer radial distribution curves for a large number of models were compared with the experimentally derived function. On this basis it was established that no significant fraction of the material in the gas phase was present in the biradical (C_{2v}) form and that the ground state has C_s symmetry. It was not possible to obtain converged solutions in the least-squares fitting of either the radial distribution or intensity functions when all the structure parameters were allowed to vary concurrently. Subject to a few constraints approximately ten models were found which were satisfactory. Fortunately these differ only slightly from each other so that a single "preferred" structure is proposed. The following interesting features appear: $C_5=C_4 = 1.350$ Å; $C_2-C_8 = 1.600$ Å; $C_1-C_5 = 1.488$ Å. The root-mean-square amplitudes of vibration for C_4-C_6 and C_2-C_8 are large; the latter is 0.11 Å; all the others are "normal." The cyclopentene rings are bent with a pucker angle of about 18°.

Tricyclo[3.3.0.0^{2,8}]octa-3,6-diene (semibullvalene) is one of several fused-ring molecules which undergoes rapid conformational inversions. For the Cope rearrangement in bullvalene the unimolecular rate constant at 0° (independent of solvent) is 790 sec⁻¹, with a corresponding activation energy of 10.9 ± 0.1 kcal/mol.¹ At the same temperature semibullvalene has a lifetime of less than 3 × 10⁻⁷ sec; the heavily substituted octamethyl derivative does have a temperature dependent nmr spectrum (-141°), from which an activation energy of about 6 kcal/mol was deduced.² The gas-phase structure for bullvalene has been studied by X-ray and electron diffraction;³ there are no corresponding structural data on semibullvalene. The present investigation has three objectives: first, to determine whether semibullvalene has a deep minimum in the potential energy function at the biradical state (C_{2v} symmetry) as it passes from one form to the other; second, if it is predominantly in the C_s form, whether the ease of inversion so characteristic of bullvalene and semibullvalene can be discerned from corresponding large root-mean-square amplitudes of vibration, such as was noted in our study of hexamethyl(Dewar benzene);⁴ finally, whether the interatomic distances found in the gas phase are in agreement with calculations made for this and similar molecules by Dewar and co-workers.^{5a} The orbital sequence in semibullvalene deduced from its photoelectron spectrum has been assigned by Askani, *et al.*^{5b}

Experimental Section

Semibullvalene was prepared from tricyclo[3.3.0.0^{2,8}]octane during the search for a synthesis of tricyclo[3.3.0.0^{2,8}]octa-3,7-diene;⁶ the latter rapidly isomerized to semibullvalene. The

sample used in the electron diffraction study was purified by preparative glpc (15% Carbowax on 60-30 Firebrick, 5 ft × 3/8 in., 100°). Its purity was established by analytical glpc and by comparison of its nmr and infrared spectra with those reported previously.⁷ The material was kept at Dry Ice temperatures except during the time that the photographs were taken, when it was raised to 50° to provide adequate vapor pressure. Two sets of diffraction photographs were obtained in the first set of experiments, and 2 weeks later another set was recorded. Diffraction patterns were first taken with the electron beam at 65 kV and a nozzle-to-plate distance of 19 cm; then with 50 kV at 25 cm; finally, a third set with 60 kV electrons at 9 cm. The sector opening was cut so as to flatten (essentially) diffraction patterns of benzene. Calibration photographs with CS₂ and MgO were recorded concurrently to provide (λ , L) values for data reduction. The procedures were slight extensions of those described in our previous publications.⁸ Figure 1 is a plot of the reduced relative intensities as a function of scattering angle q [$q \equiv 40/\lambda \sin \theta/2$]. With overlapping sections the useful range covered is $q = 10$ -147. Numerical values of the total relative intensities *vs.* q are attached to this paper in the microfilm edition.⁹

Somewhat modified computational procedures were followed in deducing the structure;¹⁰ these lean heavily on newly developed programs for the DEC PDP-9 augmented computer (outlined in Table I). The programs permit the rapid conversion of the digitized photometer punched tape output to intensities at integral q 's: introduce a semiautomatic procedure for drawing-in a background and compute a Fourier transform which is the atom-pair distance spectrum in the molecule. The final radial distribution curve is obtained in a sequence of successive approximations, wherein the positivity criterion is used, as needed, and corrections are made for the nonnuclear scattering and phase shift in the atom form factors. With the available programs any portion of the radial distribution curve may be displayed on a large CRT screen and compared with that calculated for an assumed model. The atomic coordinates are calculated from a specified set of parameters.¹¹ Changes can be inserted in the program either manually (teletype) or by seeking optimum values for selected parameters through a least-squares fitting calculation based on superposed skewed Gaussians. The

(1) A. Allerhand and H. S. Gutowsky, *J. Amer. Chem. Soc.*, **87**, 4092 (1965); G. Schröder and J. F. M. Oth, *Angew. Chem., Int. Ed. Engl.*, **6**, 414 (1967).

(2) F. A. L. Anet and G. E. Schenck, *Tetrahedron Lett.*, **48**, 4237 (1970).

(3) (a) A. Amit, R. Huber, and W. Hoppe, *Acta Crystallogr., Sect. B*, **24**, 865 (1968); (b) B. Anderson and A. Marstrand, *Acta Chem. Scand.*, **25**, 1271 (1971).

(4) M. J. Cardillo and S. H. Bauer, *J. Amer. Chem. Soc.*, **92**, 2399 (1970).

(5) (a) M. J. S. Dewar and W. W. Schoeller, *ibid.*, **93**, 1481 (1971); (b) R. Askani, *et al.*, *Tetrahedron Lett.*, **46**, 4461 (1971).

(6) J. Meinwald and H. Tsuruta, *J. Amer. Chem. Soc.*, **91**, 5877 (1969).

(7) H. E. Zimmerman, *et al.*, *ibid.*, **91**, 3316, 5878 (1969); **90**, 4763 (1968); **88**, 183 (1966).

(8) J. L. Hencher and S. H. Bauer, *ibid.*, **89**, 5527 (1967); W. Harshbarger, *et al.*, *Inorg. Chem.*, **8**, 1683 (1969); R. L. Hilderbrandt and S. H. Bauer, *J. Mol. Struct.*, **3**, 325 (1969).

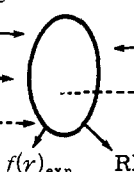
(9) An appendix will appear following these pages in the microfilm edition of this volume of the journal. Single copies may be obtained from the Business Operations Office, Books and Journals Division, American Chemical Society, 1155 Sixteenth St., N.W., Washington, D. C. 20036, by referring to code number JACS-72-5651. Remit check or money order for \$3.00 for photocopy or \$2.00 for microfiche.

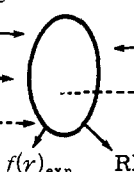
(10) S. H. Bauer and A. L. Andreassen, *J. Phys. Chem.*, in press.

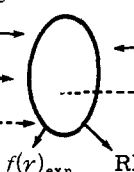
(11) R. L. Hilderbrandt *J. Phys. Chem.*, **51**, 1654 (1969).

Table I. Data Reduction (DEC PDP-9) Sequence

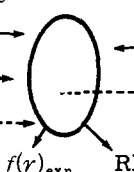
1. Convert photometer punched tape to $I(q)$; $q \equiv 40/\lambda \sin \theta/2$
 Correct for nonlinearity of density function
 Correct for planar projection of focal sphere, etc.
 Scale various densities
 Splice several ranges; average several tracings
2. Successive approximation sequence for drawing-in smooth background and for computing radial distribution curve

$\langle \text{PDP-9} \rangle_{av} I(q)$ curve \longrightarrow 

Insert matrix $\{Z_i; l_{ij}\}$ \longrightarrow 

Model (state parameters) \dashrightarrow 

Displayed on CRT (20 sec) $f(r)_{exp}$ RD (model)

$\left\{ \begin{array}{l} \text{Library of atom form} \\ \text{factors and phase angles} \end{array} \right.$ \longleftarrow 

\dashrightarrow Calcd cartesian coordinates
3. Refine background; adjust model
4. Least-squares fit of $f(r)_{exp}$ and $qM(q)$ functions

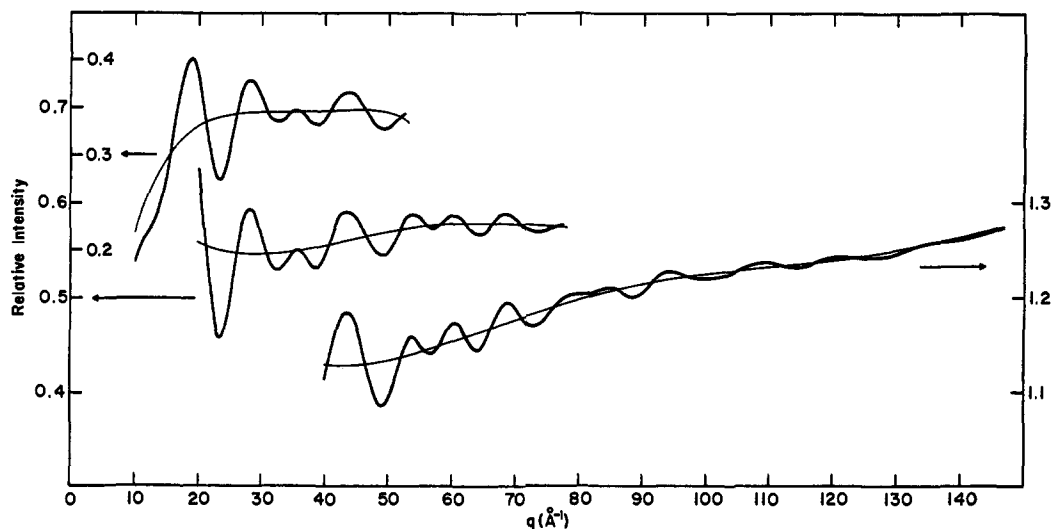


Figure 1. Reduced intensities plotted vs. $q = 40/\lambda \sin \theta/2$; the smooth lines (drawn in) are the refined backgrounds. Note the scale change for the three plots.

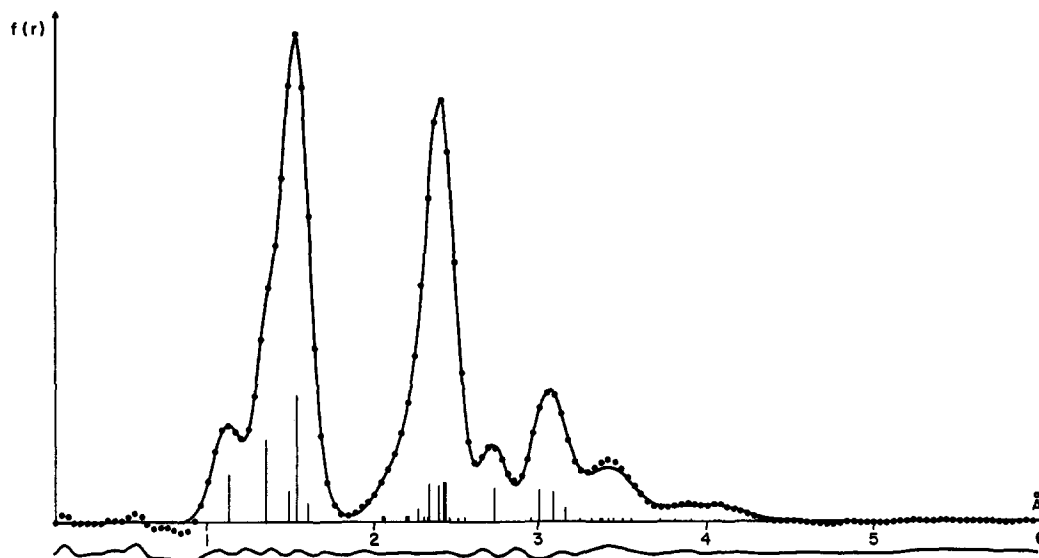


Figure 2. The experimental (dots) and final theoretical radial distribution functions. Their difference is plotted below them. Successive dots are spaced by 0.04 Å.

revised radial distribution curve is displayed on the screen within about 20 sec. In this manner a large number of trial structures can be rapidly tested. When an adequate combination of parameters is found, similar models can be investigated to determine whether the acceptable one is a unique representation of the radical distribution function. Permanent records of these curves are obtained with a digital plotter (10 min).

Analysis and Results

The radial distribution curve for the most acceptable model is shown in Figure 2. The C_s structure and a plausible biradical C_{2v} conformation were inserted as zero-order models, for comparison with the experi-

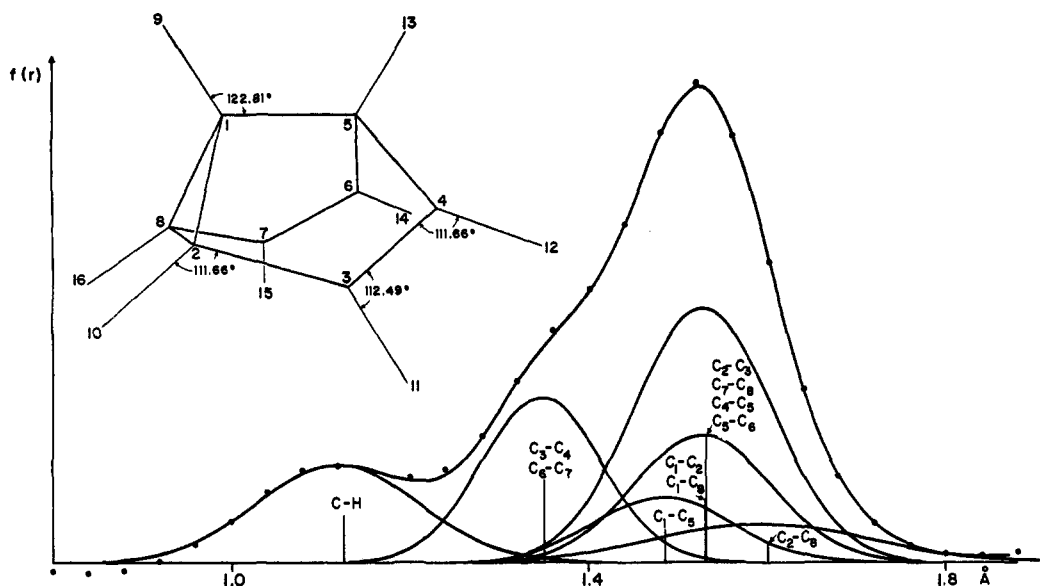
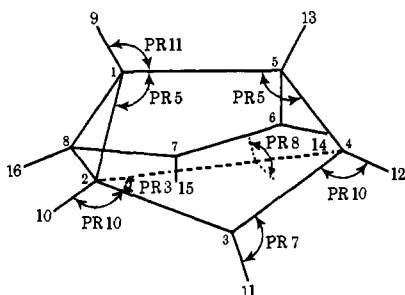


Figure 3. Components of the theoretical radial distribution function, each with the shape of a skewed Gaussian (see text). The dots indicate the experimental values. $b = 2.303(\pi q_{\max}/10)^{-2}$.

Table II. Parameters for Semibullvalene



| | |
|-------|--|
| PR 1 | C_1-C_5 |
| PR 2 | C_1-C_2 |
| PR 3 | $\angle C_4C_2C_3$ |
| PR 4 | Angle between $H_9C_1C_3H_{13}$ and $C_4C_1C_5$ |
| PR 5 | $\angle C_3C_1C_5$; $\angle C_4C_5C_1$ (assumed equal) |
| PR 6 | $\langle C-H \rangle_{av}$ |
| PR 7 | $\angle C_4C_3H_{11}$ (H_{11} was constrained to the plane of $C_2C_3C_4$) |
| PR 8 | Angle between $C_3C_3C_4$ and $C_2C_4C_5$ |
| PR 9 | Angle between $H_{10}C_2C_3$ and $C_1C_2C_3$ |
| PR 10 | $\angle H_{10}C_2C_3$ |
| PR 11 | $\angle H_9C_1C_5$ |
| PR 12 | Angle between $H_9C_1C_3H_{13}$ and $C_2C_1C_5$ |
| PR 13 | C_4-C_5 |
| PR 14 | C_2-C_3 |

Locate H_{12} ($\angle C_3C_4H_{12} = PR 10$) and $\angle (C_3C_4H_{12}$ and $C_3C_4C_6) = PR 9$

mental data. The range of intensities in q (10–87) obtained in the first two sets of photographs was not sufficient to distinguish between these starting models. The third set of patterns provided intensities to $q = 147$ and led to much better resolution in the radial distribution function. A shoulder appeared to the left of the first main peak. This clearly eliminated the possibility that a substantial fraction of the sample existed in the biradical form. Ultimately the radial distribution curve in the region 1–2 Å was resolved as shown in Figure 3. There appears to be no residuum area which might be ascribed to a significant amount of material in the biradical form. Further proof was provided by the

Figure 4. "Sharpened" radial distribution. The top curve was derived from the data; the middle one is the computed sharpened radial distribution function for the accepted model (no. 1) and the bottom curve is their difference. The "modification function" was set equal to $\exp[-\lambda(q_{\max} - q)]$, with $\lambda = 0.03$.

"sharpened" radial distribution function.¹² Figure 4 shows the $C=C$ region clearly resolved from that of the superposed $C-C$, with very little possibility that there is significant scattering at approximately 1.40–1.43 Å, anticipated for the biradical form. From this point, consideration was limited to the C_s model.

While the resolution of the bonded region (1–2 Å) is not unique, it is clear that it is necessary to introduce several somewhat short $C-C$ bonds (≈ 1.50 Å) and another long one (≈ 1.60 Å) in order to account for the overall breadth of the first large peak. The use of five different $C-C$ single bond lengths with correspondingly high correlations made the least-squares fitting of

(12) M. Traetteberg and R. A. Bonham, *J. Chem. Phys.*, **42**, 587 (1965).

Table III. Atom Pair Distances Derived from Least-Squares Fitting of the Radial Distribution Curve (Model 10)

| Typical i | Typical j | r_{ij} | No. of pairs | Σ peak height | l_{ij} | l_{ij} code |
|-------------|-------------|-------------|--------------|----------------------|----------|---------------|
| 3 | 11 | 1.125 | 8 | 587 | 0.079 | 2 |
| 6 | 7 | 1.350 | 2 | 992 | 0.050 | 5 |
| 5 | 1 | 1.485 | 1 | 393 | 0.062 | 1 |
| 1 | 2 | 1.530-1.531 | 6 | 2291 | 0.062 | 1, 4 |
| 2 | 8 | 1.600 | 1 | 234 | 0.111 | 3 |
| 7 | 14 | 2.051-2.061 | 4 | 142 | 0.092 | 9 |
| 8 | 10 | 2.189 | 2 | 66 | 0.092 | 9 |
| 14 | 15 | 2.199 | 2 | 7 | 0.145 | 12 |
| 6 | 13 | 2.199 | 2 | 66 | 0.092 | 9 |
| 4 | 6 | 2.261 | 1 | 165 | 0.111 | 3 |
| 5 | 9 | 2.298-2.321 | 4 | 126 | 0.092 | 9 |
| 5 | 3 | 2.325-2.381 | 4 | 929 | 0.069 | 7 |
| 8 | 6 | 2.411-2.421 | 6 | 1478 | 0.060 | 6 |
| 2 | 11 | 2.450-2.541 | 6 | 174 | 0.092 | 9 |
| 2 | 7 | 2.716 | 2 | 432 | 0.062 | 8 |
| 10 | 11 | 2.741-2.886 | 4 | 11 | 0.145 | 12 |
| 6 | 12 | 2.941 | 2 | 47 | 0.097 | 10 |
| 4 | 7 | 2.989-3.070 | 4 | 774 | 0.062 | 8 |
| 9 | 10 | 3.112 | 2 | 5 | 0.145 | 12 |
| 3 | 7 | 3.146 | 1 | 186 | 0.062 | 8 |
| 3 | 13 | 3.234 | 2 | 43 | 0.097 | 10 |
| 3 | 9 | 3.307-3.545 | 20 | 394 | 0.097 | 10 |
| 8 | 11 | 3.714-4.104 | 12 | 158 | 0.135 | 11 |
| 13 | 15 | 4.165-5.019 | 17 | 24 | 0.167 | 13 |

bond lengths as well as the angles. Ultimately the entire curve was fitted, as indicated in Figure 2, through the patient variation of the 14 parameters, selected as listed in Table II. In the least-squares fitting of the radial distribution curve, it was not possible to obtain a converged solution when all the bonded C—C lengths were allowed to vary independently; however, by inserting the condition that selected pairs of C—C separations were equal (ten models were tested), converged solutions for sets of parameters were deduced with an overall fit to within $R = 2.2\%$.

$$R_f \equiv \frac{\sum_r |f_c - f_x|}{\sum_r f_x}; \quad \Delta r = 0.04 \text{ \AA}$$

f_c, f_x are the calculated and experimental radial distribution functions, respectively. In these calculations the root-mean-square amplitudes were assigned at reasonable values, as listed in Table III. The ten models are characterized as shown in Table IV. Acceptable converged solutions were found for all these models. The corresponding parameters are given in Table V. With the possible exception of model 2, the electron diffraction data do not clearly favor one over the other. There is no unambiguous dividing line be-

Table IV

| Model | | |
|-------|------------------------------------|-------------------------------------|
| 1 | (1-2) = (4-5) = (2-3) | PR 2 = PR 13 = PR 14 |
| 2 | (1-5) = (1-2) = (4-5) | PR 1 = PR 2 = PR 13 |
| 3 | (1-5) = (2-3); (1-2) = (4-5) | PR 1 = PR 14 and PR 2 = PR 13 |
| 4 | (1-5) = (1-2); (4-5) = (2-3) | PR 1 = PR 2 and PR 13 = PR 14 |
| 5 | (1-5) = (4-5); (1-2) = (2-3) | PR 1 = PR 13 and PR 2 = PR 14 |
| 6 | (1-2) = (4-5); (2-3) = 1.5332 \AA | PR 2 = PR 13 and PR 14 = 1.5332 \AA |
| 7 | (1-2) = (4-5); (2-3) = 1.5321 \AA | PR 2 = PR 13 and PR 14 = 1.5321 \AA |
| 8 | (4-5) = 1.5299; (2-3) = 1.5321 \AA | PR 13 = 1.5299; PR 14 = 1.5321 \AA |
| 9 | (4-5) = 1.5295; (2-3) = 1.5321 \AA | PR 13 = 1.5295; PR 14 = 1.5321 \AA |
| 10 | (4-5) = 1.5309; (2-3) = 1.5309 \AA | PR 13 = 1.5309; PR 14 = 1.5309 \AA |

Table V. Least-Squares Values for 11 Models [$f(r)$ curves]

| Model | 1 | 2 | 3 | 4 | 5 | 6 | 7 | 8 | 9 | 10 | 11 |
|---|---------|---------|---------|---------|---------|--------|---------|--------|--------|---------|--------|
| PR 1 C ₁ -C ₅ | 1.4832 | 1.5127 | 1.5073 | 1.5020 | 1.5044 | 1.4844 | 1.4853 | 1.4858 | 1.4852 | 1.4849 | 1.4879 |
| 2 C ₁ -C ₃ | 1.5309 | 1.5127 | 1.5351 | 1.5020 | 1.5384 | 1.5295 | 1.5299 | 1.5293 | 1.5298 | 1.5299 | 1.5333 |
| 3 \angle C ₄ C ₃ C ₂ | 30.87 | 31.20 | 30.90 | 30.94 | 30.98 | 30.87 | 30.88 | 30.88 | 30.87 | 30.89 | 30.87 |
| 4 | 129.54 | 128.97 | 129.92 | 129.81 | 128.36 | 129.44 | 129.48 | 129.48 | 129.44 | 129.53 | 129.60 |
| 5 \angle C ₂ C ₁ C ₃ | 106.85 | 106.38 | 106.09 | 106.61 | 106.34 | 106.84 | 106.80 | 106.80 | 106.81 | 106.80 | 106.67 |
| 6 \langle C—H \rangle_{av} | 1.1251 | 1.1251 | 1.1223 | 1.1206 | 1.1227 | 1.1248 | 1.1248 | 1.1248 | 1.1248 | 1.1251 | 1.1253 |
| 7 \angle C ₄ C ₃ H ₁₁ | 111.57 | 134.68 | 113.83 | 115.68 | 113.78 | 111.74 | 112.38 | 112.07 | 112.06 | 112.49 | 113.25 |
| 8 | 181.99 | 179.51 | 183.50 | 182.11 | 180.55 | 181.85 | 181.98 | 181.79 | 181.80 | 181.95 | 182.53 |
| 9 | 175.53 | 182.06 | 175.18 | 173.81 | 173.78 | 175.43 | 174.91 | 175.27 | 175.33 | 175.03 | 174.19 |
| 10 \angle H ₁₀ C ₂ C ₃ | 112.51 | 105.98 | 112.84 | 110.85 | 111.78 | 112.79 | 11.193 | 112.30 | 112.46 | 111.66 | 113.74 |
| 11 \angle H ₉ C ₁ C ₅ | 112.13 | 124.59 | 124.50 | 124.09 | 123.43 | 121.85 | 122.87 | 121.45 | 121.74 | 122.81 | 121.18 |
| 12 | 146.92 | 146.83 | 146.82 | 146.49 | 147.36 | 146.97 | 146.96 | 146.91 | 146.94 | 146.90 | 147.03 |
| 13 C ₄ -C ₅ | 1.5309 | 1.5127 | 1.5351 | 1.5392 | 1.5044 | 1.5295 | 1.5299 | 1.5299 | 1.5295 | 1.5309 | 1.5214 |
| 14 C ₂ -C ₃ | 1.5309 | 1.5529 | 1.5073 | 1.5392 | 1.5384 | 1.5332 | 1.5321 | 1.5321 | 1.5321 | 1.5309 | 1.5309 |
| C ₃ =C ₄ | 1.3495 | 1.3468 | 1.3483 | 1.3459 | 1.3477 | | 1.3493 | | | 1.3495 | |
| C ₂ -C ₈ | 1.5996 | 1.5881 | 1.6145 | 1.5894 | 1.5923 | | 1.5971 | | | 1.5996 | |
| $R_f, \%$ ^a | 2.263 | 2.724 | 2.659 | 2.698 | 2.646 | 2.289 | | 2.301 | 2.295 | 2.225 | 2.300 |
| $R_q, \%$ ^b | 7.595 | 9.069 | 8.258 | 8.554 | 8.366 | | 7.683 | | | 7.608 | |
| $\sigma_q, \%$ ^c | 0.02742 | 0.03136 | 0.02965 | 0.03088 | 0.02965 | | 0.02763 | | | 0.02734 | |

^a R_f , residual derived for fitting the radial distribution curve. ^b R_q , residual derived for fitting the $qM(q)$ curve. ^c σ_q , standard deviation derived from fitting of the $qM(q)$ curve.

this peak in the radial distribution curve quite difficult. Similarly the assignment of bond angles as dictated by the region from 2 to 3 \AA also is not unique, but the combined peaks from 1 to 3 \AA placed constraints on the

tween R factor of 0.027 for no. 2 and $R = 0.022$ for no. 10. It is worth noting, however, that with the exception of model 2, values for the deduced parameters differ very little from each other. We discarded model

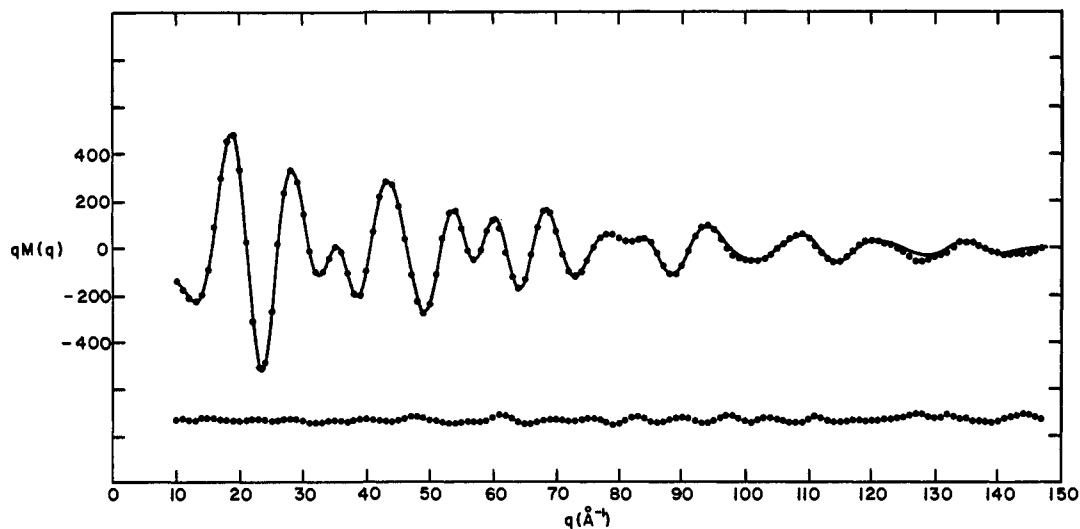


Figure 5. The experimental (dots) and the theoretical $qM(q)$ curves ("best" model). The lower curve is the difference function.

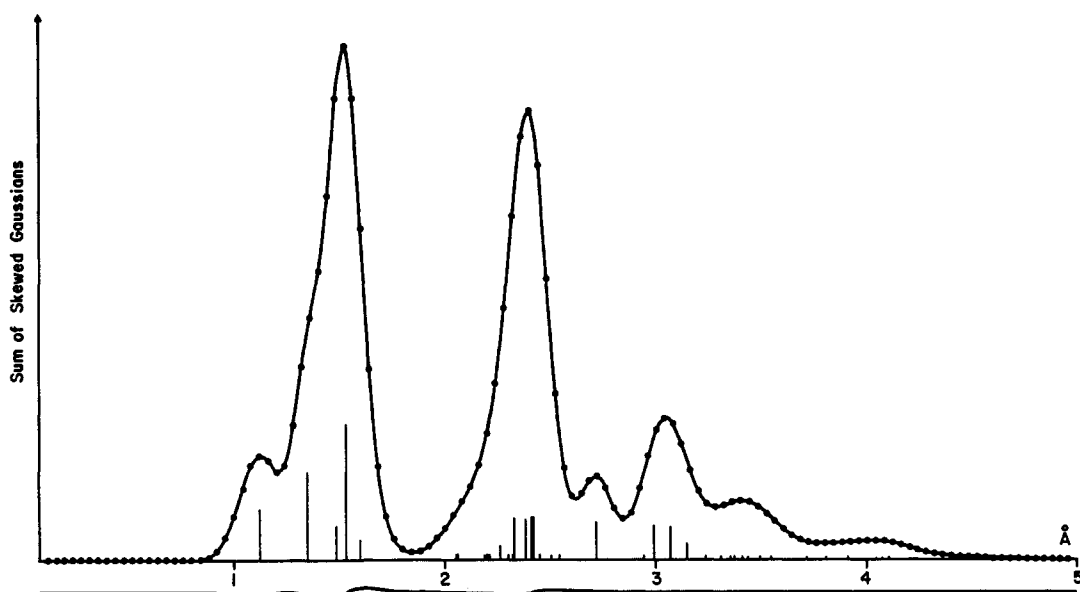


Figure 6. The points indicated the radial distribution function obtained by inversion of the calculated $qM(q)$ function, for model no. 1, following the conventional procedure, and the solid curve is that obtained by superposition of skewed Gaussians for that model. The lower curve is the difference between them.

2 (see justification below) and propose no. 1 as preferred.

The reduced molecular intensity scattering is shown in Figure 5. The final set of parameters for semibullvalene was obtained by least-squares fitting the calculated $qM(q)$ curve to that observed, using the l_{ij} 's listed in Table VI. The converged values are given along with the corresponding error limits assigned at three times the standard deviations (justification in ref 9) calculated in the reduction of the intensity data. Our experience with this structure determination is that fitting the radial distribution curve was an easier process than fitting the molecular intensity pattern, that the inherent nonuniqueness of one-dimensional Fourier transforms limits the specification of detailed geometry for large molecules with low symmetry, and that the solution may depend on the test models inserted in the data reduction process.

Inspection of Table V shows that for none of the models could all 14 geometrical parameters be varied concurrently to achieve a converged solution by least squares. In each case either it was necessary to constrain two or more highly correlated parameters so that they were equal or to assign them to a constant value. However, for all the combinations which did lead to a good fit with the experimental radial distribution, C_1-C_5 ranged from 1.483 to 1.513 Å; C_1-C_2 from 1.502 to 1.535 Å; C_4-C_5 from 1.504 to 1.535 Å; and C_2-C_3 from 1.507 to 1.553 Å. In every case C_1-C_5 is either the shortest or one of the shortest single bonds in the molecule. The distances C_1-C_2 and C_4-C_5 show a high correlation in the least-squares analysis. The best values for both appear to be 1.530 Å. Whereas C_2-C_3 was almost equal to C_1-C_2 and C_4-C_5 , consideration of the R and σ values indicated

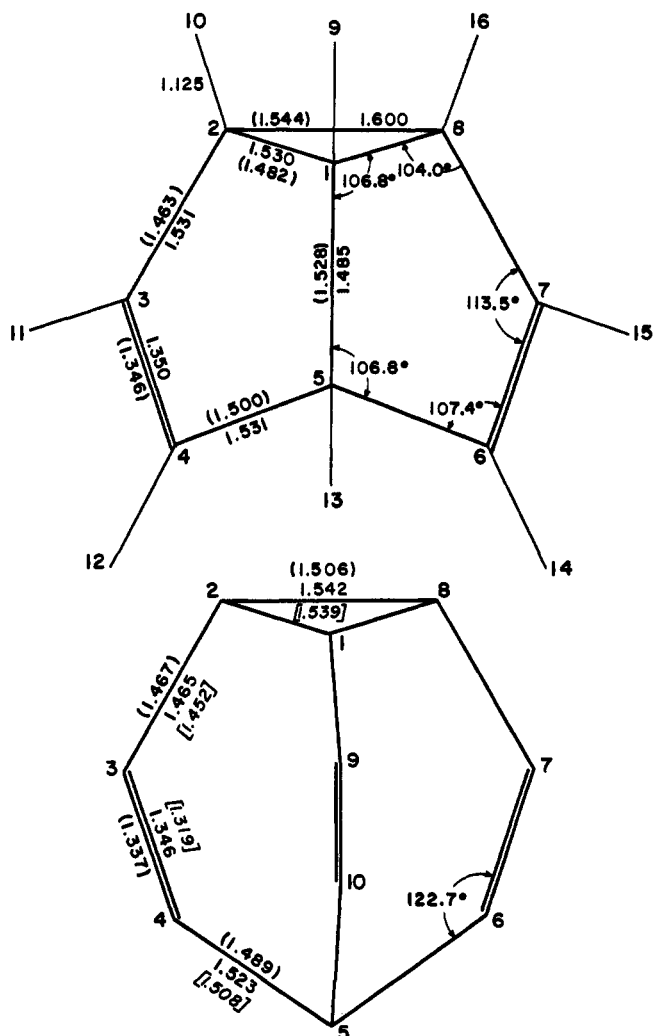


Figure 7. Semibullvalene projected onto a plane. The dimensions given are those derived for model no. 1; the values in parentheses are those calculated by Professor Dewar.¹³ For comparison, recall that in bullvalene the C_1-C_5 bond is replaced by a $-C=C-$ group, so that correspondence is limited. The lower projected figure for bullvalene is distorted somewhat with values given by Amit, *et al.*,^{3a} and by Anderson, *et al.*^{3b}

Table VI. Least-Squares Fitting of $qM(q)$ Values^a

| | | | | | |
|-----------|----|-------------------|----------|----|-------------------|
| PR | 1 | 1.477 ± 0.018 | l_{ij} | 1 | 0.076 ± 0.008 |
| | 2 | 1.533 ± 0.004 | | 2 | 0.082 ± 0.009 |
| | 3 | 30.76 ± 0.27 | | 3 | 0.111^b |
| | 4 | 130.4 ± 0.67 | | 4 | 0.041 ± 0.007 |
| | 5 | 107.3 ± 0.41 | | 5 | 0.054 ± 0.009 |
| | 6 | 1.128 ± 0.009 | | 6 | 0.058 ± 0.004 |
| | 7 | 111.6^b | | 7 | 0.061 ± 0.007 |
| | 8 | 185.7 ± 3.0 | | 8 | 0.056 ± 0.004 |
| | 9 | 175.5^b | | 9 | 0.088 ± 0.014 |
| | 10 | 112.5^b | | 10 | 0.084 ± 0.005 |
| | 11 | 122.1^b | | 11 | 0.135 ± 0.013 |
| | 12 | 147.3 ± 0.40 | | 12 | 0.105 ± 0.07 |
| | 13 | 1.531^b | | 13 | 0.163 ± 0.06 |
| | 14 | 1.531^b | | | |
| $C_3=C_4$ | | 1.358 | | | |
| C_2-C_8 | | 1.582 | | | |

^a Code for PR 1...14 given in Table II; code for l_{ij} 1...13 given in Table III. ^b Fixed during final least-squares calculation.

that models in which C_2-C_3 was somewhat longer were favored.

The deduction of acceptable models for this compound rests on the use of the "skewed Gaussian ap-

proximation" in calculating radial distribution curves, for comparison with the Fourier transform of the scattered intensity. Indeed, for structures which have several groups of nearly equal atom-pair distances, as are present in semibullvalene, the least-squares reduction of the $qM(q)$ function is of limited value. Nearly half of the parameters required to specify the structure must be constrained in order to obtain convergence. However, adjustment of the calculated to the experimental radial distribution is rapidly checked by viewing the patterns on the CRT screen and allows the exploration of the full range of parameters. Is the superposition of skewed Gaussians for all atom-pair contributions

$$f_{ij}(r) = (\text{no. of pairs}) \frac{Z_i Z_j}{r} \left(\frac{\pi}{2l_{ij}^2 + 4b} \right)^{1/2} \times \exp[-(r - r_{ij})^2 / (2l_{ij}^2 + 4b)]$$

where b is chosen such that $\exp(-bs_{\text{max}}^2) = 0.1$, a good approximation to the Fourier transform of the intensity? To answer this question, the calculated $qM(q)$ curve for model no. 1 was inverted and compared with the sum of skewed Gaussians in Figure 6. Over the range 0-5 Å, the R factor for this pair is 0.75%, which is $1/3$ of the discrepancy between the calculated and experimental curves. We concluded that the superposition of skewed Gaussians for all atom-pair contributions is an adequate approximation for this and similar structures. Clearly, the approximation is not appropriate for molecules which have free internal rotations.

Discussion

A drawing of the structure projected onto a plane, with inscribed interatomic distances and bond angles as deduced from the least-squares fitting of the skewed Gaussian radial distribution function, is shown in Figure 7. Since the correspondence between the experimental and calculated curves, both for the diffraction data and its Fourier transform, is good by present standards, we believe that our first question (whether semibullvalene has a deep potential energy minimum at the biradical state) was answered in the negative. The coplanarity of $C_2C_3C_4C_5$ was considered as a parameter (PR8) and allowed to vary during the least-squares analysis. As indicated in Table V, the largest departure appears in model 3; it is 3.5° from a planar structure. However, C_1 clearly cannot be in the plane of $C_2C_3C_4C_5$. The pucker angle between $C_1C_2C_5$ and $C_2C_4C_5$ is 17.6° ; between $C_1C_2C_5$ and $C_2C_3C_5$ it is 18.6° . The corresponding angle in perfluorocyclopentene is 21.9° and in cyclopentene it is 29.0° .

All the l_{ij} 's listed in Table III except those which correspond to the pairs C_2-C_3 and C_4-C_6 are within the usual range for hydrocarbons. It is not as certain that C_4-C_6 has a large root-mean-square amplitude because its contribution to the second main peak is relatively small. However, C_2-C_8 clearly contributes the tail of the first main peak and its amplitude is obviously large; see Figure 3. The dynamics of rapid inversion are apparent in the thermally averaged structure, as seen by electron diffraction.

Several unexpected features do appear in the final structure. The bridge C_1-C_5 is a short single bond at 1.49 Å. While we anticipated a somewhat large value for the labile bond C_2-C_8 , the one deduced proved to

be greater than expected. It does have a large root-mean-square amplitude of 0.11 Å. Prepublication calculations by Dewar and Bodor¹³ are given in brackets in Figure 7. Agreement for C₃—C₄ and C₂—C₈ is excellent; for C₄—C₅ it is adequate, since the calculated values often are 0.01–0.02 Å short. However, the comparison for C₁—C₅, C₁—C₂, and C₂—C₃ is disturbing, in that their relative orders appear to be inverted. Models in which C₁—C₅ was constrained to be larger than C₂—C₃ were tested extensively but no suitable combination of parameters was found which gave an acceptable *R* value.

The assignment of classical orbitals to this molecule is not appropriate since these suggest no rationale for the observed rapid interconversion. Note that C_s symmetry provides two A₁ and two A₂ molecular orbitals for the p electrons on C₃, C₄ and C₆, C₇. One each of the A₁ and A₂ MO's serve as two π-bonding orbitals, and the other two provide two π-antibonding orbitals. If these are the only π orbitals in the molecule, to excite

(13) Professor M. J. S. Dewar and Dr. Nicholas Bodor; many thanks for private communication.

them or to break a σ bond would require an energy of the order of 80 kcal. Hence a Walsh-like model¹⁴ must be introduced to describe the bonding situation around C₁, C₂, C₈, which must be modified to show greater overlap at C₁C₂ and C₁C₈ than at C₂C₈. One must allow for a similar description for the anticipatory cyclopropene ring at C₄, C₅, C₆; these would have to contribute (in part) two p orbitals that are not directly involved in the bonding of the hydrogens in the direction perpendicular to the σ-orbital plane. This suggests some π–π overlap for the C₁—C₅ bond, giving it the appearance of the central bond in butadiene.

Acknowledgment. This work was supported partly by the National Science Foundation under Grant No. GP-7794 and the Advanced Research Projects Agency (Material Science Center, Cornell University, Ithaca, N. Y.). Our sincere thanks to Professor J. Meinwald, J. T. Slama, and J. A. Kapecki for the sample of semibullvalene and to Professor Dewar and Dr. Bodor for their prepublication structure.

(14) W. A. Bennett, *J. Chem. Educ.*, **44**, 17 (1967).

Use of a Spectral–Solubility Method in Studies of Molecular Complexes of Iodine

Jerry D. Childs,^{1a} Sherril D. Christian,*^{1a} and Just Grundnes^{1b}

*Contribution from the Departments of Chemistry,
The University of Oklahoma, Norman, Oklahoma 73069,
and the University of Oslo, Blindern, Oslo 3, Norway.
Received November 19, 1971*

Abstract: A convenient spectral–solubility method has been developed for inferring thermodynamic constants and spectral band parameters for molecular complexes of iodine; solid mixtures of tetramethylammonium pentaiodide and tetramethylammonium triiodide serve as constant activity sources of iodine. The technique has been used to infer formation constants and extinction coefficients of visible and ultraviolet bands of complexes of iodine with the electron donors benzene, diethyl ether, and pyridine in the solvent heptane. Results are compared with those obtained using conventional spectral methods. The polyiodide solubility method is shown to have several important advantages over purely spectral techniques particularly in the study of relatively weak molecular complexes.

The Benesi–Hildebrand equation and related expressions have been widely used in obtaining spectral and thermodynamic parameters characteristic of 1:1 electron donor–acceptor (EDA) complexes of iodine and other acceptors.^{2–4} However, these methods are subject to criticism, particularly regarding their utility in studies of weak molecular complexes.

(1) First of all, in using spectral methods to study complex formation, it is necessary to infer two parameters from a set of spectral measurements at various concentrations—the equilibrium constant for formation

of the complex (K_c) and the extinction coefficient (ϵ) of a spectral band having an absorbance which varies in direct proportion to the concentration of the molecular complex. Although the product ϵK_c can be determined from measurements restricted to the dilute region, resolution of the product into separate values of K_c and ϵ requires spectral measurements extending into concentration ranges in which a sizable fraction of the least concentrated reacting solute (usually the acceptor) is in the complexed form.⁵ Thus, in studies of complexes for which K_c is considerably less than 1 l. mol⁻¹, it is necessary to use solute concentrations well in excess of 1 *M*. At such concentration levels, the medium is hardly equivalent to pure solvent; in fact it may be expected that both the spectral and the thermodynamic

(1) (a) University of Oklahoma; (b) University of Oslo.
(2) (a) R. S. Mulliken and W. B. Person, "Molecular Complexes," Wiley-Interscience, New York, N. Y., 1969; (b) G. Briegleb, "Elektronen-Donator-Acceptor-Komplexe," Springer-Verlag, Berlin, 1961.
(3) R. Foster, "Organic Charge-Transfer Complexes," Academic Press, London and New York, 1969.
(4) R. L. Scott and D. V. Fenby, *Annu. Rev. Phys. Chem.*, **20**, 111 (1969).

(5) (a) W. B. Person, *J. Amer. Chem. Soc.*, **87**, 167 (1965); (b) D. A. Deranleau, *ibid.*, **91**, 4044 (1969).